Quantitative bedform analysis using decimetre resolution swath bathymetry

Pierre W. Cazenave [*]   David O. Lambkin [†]   Justin K. Dix [*]

September 5, 2008

Abstract

Quantifying the seabed in natural environments has received little attention in spite of these characteristics being regularly cited as important features in the identification of sediment transport direction and magnitude. Classification schemes have been developed which group similar types of bedforms from distinct aquatic environments together based on wavelength, amplitude, orientation, planform and slope.

Here, we analyse a swath bathymetry surface from the Hastings shingle bank using qualitative interpretation techniques applied to illuminated bathymetry and 2-D slope and aspect maps generated using GIS software tools.

In addition, we present a Fourier transform based technique to quantify the wavelength, amplitude and orientation of 2-D bathymetric surfaces collected with multibeam sensors. The technique is tested on synthetic beds with known parameters in order to establish its ability to correctly extract multiple factors. A 1 m resolution bathymetric data set from the Hastings shingle bank of uniform bedforms is analysed using the technique to show the actual variability in natural environments.

1   Introduction

Decimetre accuracy multibeam swath bathymetry systems with metre-horizontal and centimetre-vertical resolution are popular because they provide cost-effective, rapid and accurate mapping of submerged environments. The bathymetric detail these systems provide represents an opportunity to apply quantitative analytical techniques to the seabed over large areas in order to better constrain the trends observed in the seabed morphology and the local hydrodynamic regime.

Traditional analyses of seabed data have relied upon qualitative interpretations of the physical characteristics of the bed, such as bedform wavelength, height and orientation. Indeed, classifications schemes have been developed to categorise the different types of bedform observed on the seabed based on their physical characteristics, where the classification and nomenclature of wave-type bedforms are typically based on wavelength, amplitude, and planform (Ashley, 1990). Quantitative analysis of the variability of the seabed has been the subject of a number of studies. Studies vary from the migration rates of dune crests in nature (Knaapen et al., 2005) and in flumes (Cataño-Lopera and García, 2006) to identifying new bedform types (Knaapen et al., 2001) to bedform classification schemes (Mitchell and Hughes Clarke, 1994) to the creation of models of wave interaction with the bed (Davis et al., 2004). To the authors' knowledge, there have been no studies which look at quantifying the characteristics of naturally occurring bedforms with a view to classification.

Quantitative 2-D spatial and temporal analyses of large scale oceanic waves in remote sensing physical oceanography data (Challenor et al., 2001; Cipollini et al., 2006) provide techniques for

---

[*]National Oceanography Centre, Southampton, SO14 3ZH, UK.

[†]ABP Marine Environmental Research Ltd., Southampton, SO14 2AQ, UK.

the calculation of two parameters often cited as defining characteristics of bedforms found in coastal waters: wavelength and amplitude. In addition, given the 2-D spatial analysis possible, the orientation of regular bedforms can be quantified.

Bedform orientation and sediment transport direction have been shown to be closely linked (Rubin and Hunter, 1987; Rubin and Ikeda, 1990). Monitoring sediment mobility is an important part of many aspects of the coastal system. At present, determining the direction of transport has been directly linked to bedform orientation, but the techniques used to determine the bedform orientation and wavelength rely on subjective measurements. Here, we present a technique to measure bedform orientation, amplitude and wavelength using a 2-D Fourier transform applied to swath bathymetry data. Estimates of error are calculated from the standard deviation of the 2-D Fourier transform spectrum, giving an indication of natural bedform variability over various different types of seabed. Knowing the orientation of a bedform field allows more traditional analyses of slope and wavelength to be undertaken with greater confidence in potential errors arising from misalignment of a transect. These new techniques will be demonstrated using data collected using a RESON SeaBat 8101 over the Hastings shingle bank in the eastern English Channel.

2   Data acquisition and processing

The Hastings shingle bank is located in the eastern English Channel and is a relict, sedimentary feature formed in the late Holocene 10,000 years BP (Hamblin et al., 1992). Regional sediment distribution is predominantly sandy gravel and sand (Grochowski et al., 1993); local sediment distribution within the survey area shows a coarse shallow bank of material surrounded by finer sands in deeper water north and south. Sediment transport on the bank is generally limited to a veneer of fine material (grain size <1 cm) moving over the coarse lag material (2-6 cm grain size) forming the body of the bank (Dickson and Lee, 1973). The tidal axis is 53° from north, and flow speeds are < 1.4 ms^{-1} (flood) and < 0.9 ms^{-1} (ebb). Data from the Channel Coastal Observatory's Pevensey Bay buoy (approximately 25 km north west of the survey site) show surface waves propagate from the south-west, with significant wave heights generally < 1.5 m, but rising as high as 3.5 m in winter.

Swath bathymetry data were collected in the summer of 2005 on board the Kommander Iona by UTEC. The data were imported into CARIS HIPS and calibration was undertaken prior to filtering beams and depths outside the survey range. A tidal correction was applied based on the data collected by a seabed pressure sensor deployed near the survey site. All depths are relative to Admiralty Chart Datum at Hastings (approximately 40 km north of the survey site). Subsequent manual cleaning was undertaken using the subset editor to remove erroneous points. Gridding resolution for the bathymetry data was chosen based on iterative gridding at increasingly fine resolutions. Once the iterative process identified a resolution where gaps were minimal, statistical analysis of the number of points contributing to a single value was undertaken to ensure every depth was the result of more than one raw value. Figure 1 shows the final cleaned surface gridded at 1 m resolution.

3   Traditional quantitative analysis

The quantitative analysis of echosounder profiles of seabed depth has been used since the advent of sonar imaging systems (e.g. Kenyon, 1970; Kenyon et al., 1981; Stride, 1982). These analyses allowed wavelength and amplitude to be measured from the paper trace record printed during acquisition, and formed some of the seminal work on coastal shelf morphodynamics.

Advances in sonar technology and digital storage mean that most measurements can now be undertaken computationally, with a larger number of samples, allowing greater accuracy, precision and confidence in the final results. However, 2-D seabed profiles through a bedform
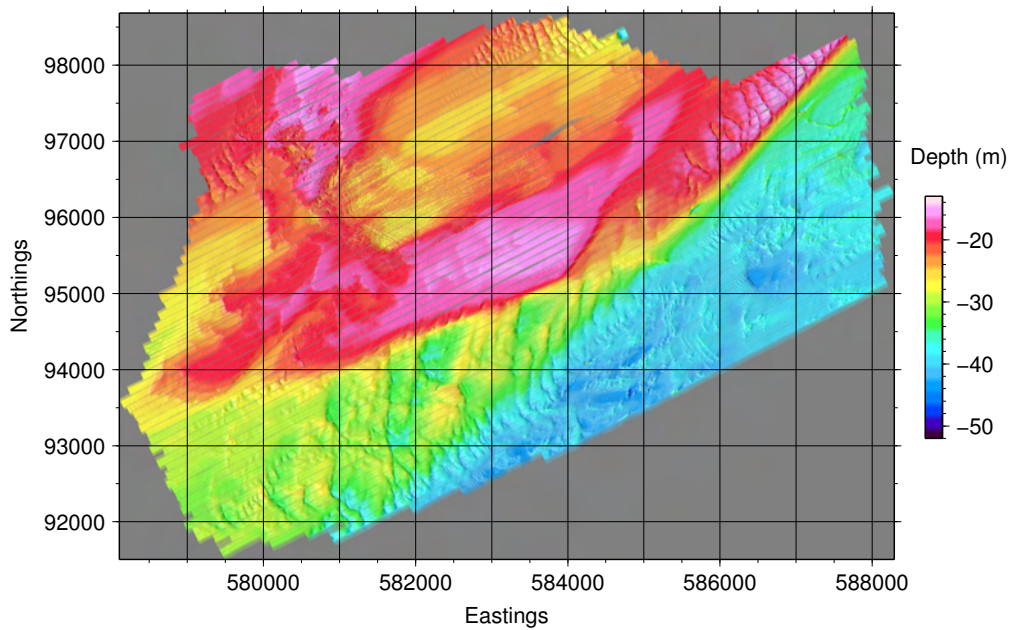
Figure 1: CARIS processed swath bathymetry gridded at 1 m showing South west illuminated bathymetry.

field still rely on the assumption that the orientation of the bedforms is known and constant along the length of the profile. Should a profile be taken through a bedform field obliquely, the resultant wavelengths would be longer than if they had been taken perpendicular to the axial orientation.

The 2-D surface generated by a swath bathymetry sensor means that the orientation of a profile is no longer governed by the direction the vessel was travelling in during echosounder acquisition. Instead, sampling a 2-D bathymetric surface is possible in any number of orientations. Given the many possible orientations, to calculate the wavelength and amplitude of a series of bedforms correctly, it is important to know their orientation. This can be achieved through a standard 2-D analysis of slope magnitude and the slope aspect applied to a swath bathymetry data set using GIS software. This calculates the gradient vector of the surface, from which slope and aspect can be extracted. de Smith et al. (2007) describes the various techniques for determining the gradient of a spatial dataset.

The slope and aspect maps shown in Figures 2a and 2b respectively are the output from the gradient analysis of the bathymetric surface shown in Figure 1. Using these two results in combination with the illuminated swath bathymetry image allows for a comprehensive qualitative interpretation of the features seen on the bed (Figure 2c).

Most modern GIS software packages (ArcGIS, MapInfo, Surfer, ERDAS Imagine, GRASS, GMT etc.) are capable of calculating the gradient vector (from which slope and aspect can be extracted) using a number of different techniques. These each attempt to address the issues which arise from using rectilinear grids.

Interpreting the bedforms within a given subset as responsible for the maximum bed slope angles, a simple plot of aspect versus slope gives the orientation of the peak slopes. For the entire Hastings shingle bank, Figure 3 shows this relationship. Three principal peaks can be identified in Figure 3: a large peak at around 55°, with maximum slope values of 35°; and a pair separated by 180° at 150° with maximum slope values of around 28°. These results show how the bank region is dominated by a large number of sloping features of ∼28° orientated 150° from north,
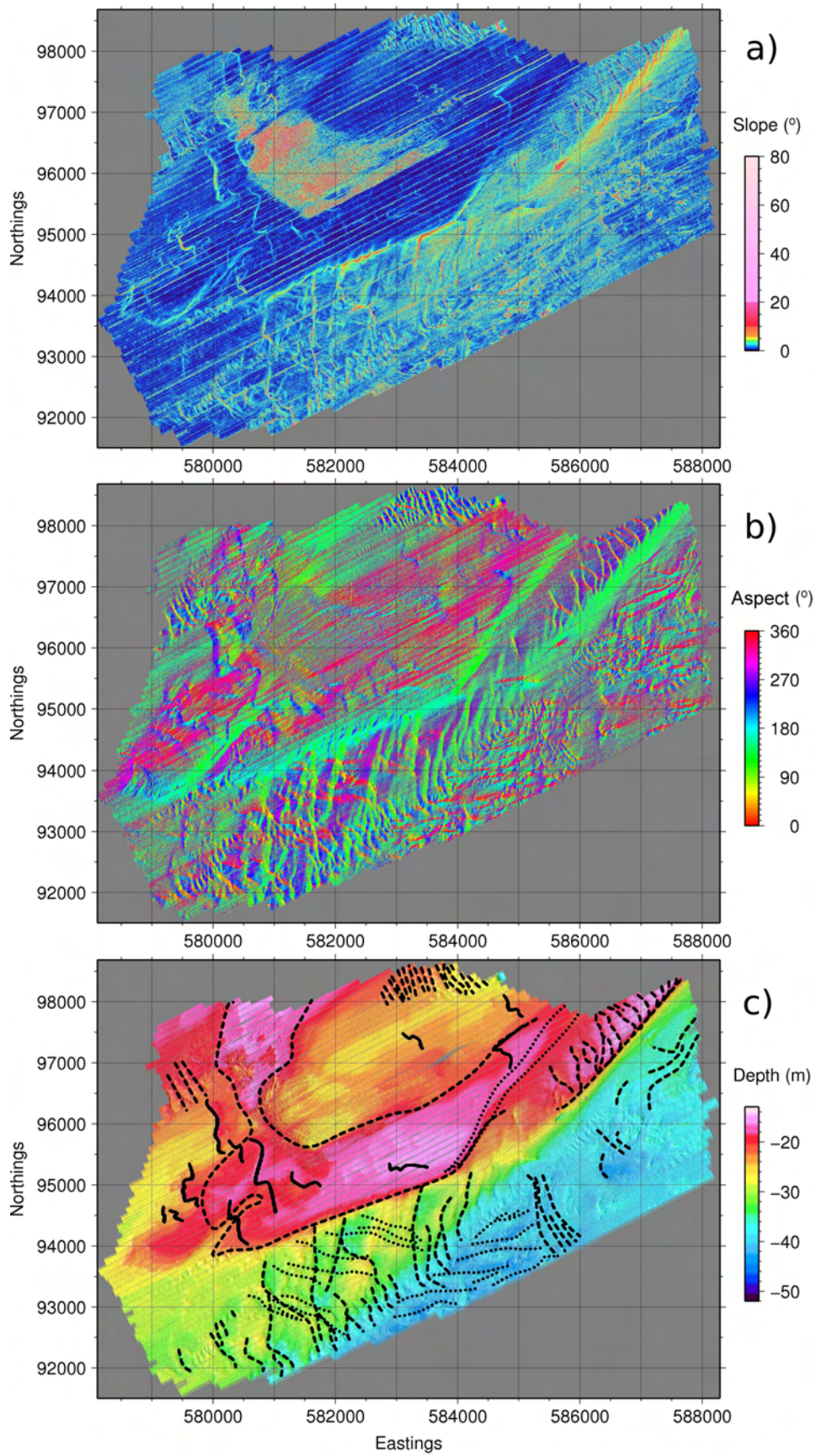
Figure 2: CARIS processed swath bathymetry analysis gridded at 1 m showing: a) Maximum bed slope angle (°). b) Maximum slope aspect in degrees from north. c) Bathymetry with overlaid interpretation based on illuminated bathymetry (dashed line), maximum bed slope angle (solid line) and slope aspect (dotted line).

4

but there is also a large number of higher slopes ($\sim 35°$) whose orientation is perpendicular to this ($\sim 60°$). Given the presence of a large aggregate extraction licence area in the centre of the bank (see Figure 1) where the majority of the dredging artefacts are orientated along the tidal axis (53°from north) to facilitate extraction, the aspect and slope analysis has identified this trend. In addition, the large number of medium dunes over the north-west, north-east and south-east of the survey area are interpreted as the other two peaks in Figure 3, and appear orientated between 140-160°.

There is still uncertainty associated with grouping all the aspect values for a given domain, but this analysis helps generate objective results with which to sample the seabed. This information can be used to calculate the start and end coordinates of a profile which is orientated perpendicular to the identified bedform orientation value. This preliminary step allows for more accurate calculations of wavelength and amplitude.

There is scope to explore the distribution of the slope magnitudes for each peak of the bedforms at $\sim 150°$ in order to identify any potential asymmetry in the distribution of the maximum slopes, and thus infer bedform asymmetry.
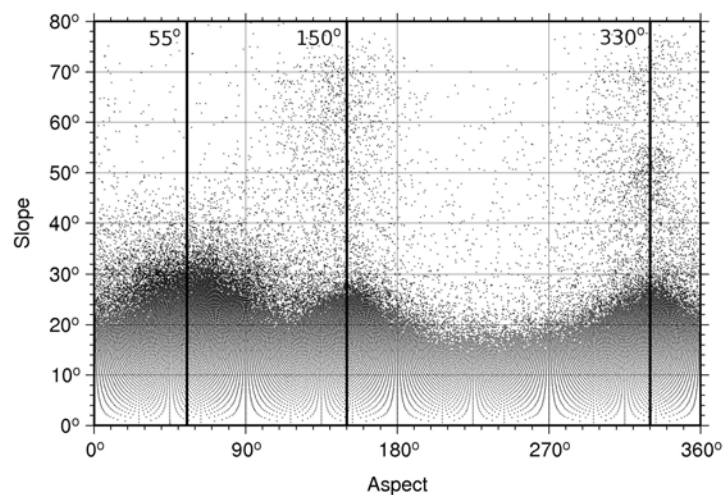

Figure 3: Slope aspect plotted against slope magnitude. Lines indicate orientations of peak bed slope.

4 Fourier transform

4.1 1-D Fourier transform

Given a 2-D profile of the seabed through a bedform field, a manual approach to characterising bedform wavelength and amplitude can be adopted by measuring the distance between peaks, and between a peak and adjacent trough to calculate the mean wavelength and amplitude of bedforms. This approach is difficult to apply and ensure a robust result is obtained, since the orientation of the transect implies a correct identification of the bedform orientation. However, techniques more commonly used in satellite-based large-scale oceanic wave identification (e.g. Cipollini et al., 1998, 2006; Challenor et al., 2001) when applied to bathymetry data can extract these values from the seabed bedforms. They provide quantitative measurements, with errors, based on measured variability and limits imposed by the relationship between the grid resolution and the minimum wavelength which can be detected (the Nyquist frequency). The domain size

input into the Fourier transform limits the wavelength of bedforms which can be calculated. The Nyquist frequency is defined as being half the domain size when considered in the spatial domain.

Equation 1 shows the continuous 1-D Fourier transform.

$$F(\nu) = \int_{-\infty}^{\infty} f(t)e^{-2\pi\nu it}\delta t \tag{1}$$

where ν is the frequency (m^{-1}), $f(t)$ is the signal in space (metres) and i is $\sqrt{-1}$.

However, since a seabed profile is not continuous (infinite), the spectrum can be approximated using the discrete Fourier transform instead:

$$A_n = \frac{1}{N} \sum_{k=0}^{N-1} a_k e^{-2\pi ink/N} \tag{2}$$

where $n = 0, 1, 2, \ldots, N - 1$, A_n is N Fourier coefficients of N values of the sequence $\{a_k\}$.

To illustrate, if applied to a 2-D profile of a synthetic seabed (see Figure 4) with a wavelength of 20 m and an amplitude of 4 m such as Figure 5a, the resultant power spectrum peaks (Figure 5b) show wavenumber, K (number of bedform wavelengths per metre), and half the amplitude of the input data. Since the input wavelength is 20 m, the equivalent wavelength expressed as K is 0.05.

The output of a Fourier transform, whether single- or multi-dimensional, always comprises a positive and negative component. Hence, all the figures of power against wavenumber (K) have two peaks which mirror one another about zero in each dimension (x and/or y). For ease of understanding, only the peaks in the positive parts of the plots are used to interpret the results.

A threshold value of 60% of the maximum amplitude is used in order to distinguish the peaks identified in Figure 5b from the background noise, which is more significant in bathymetric data than the clean synthetic dataset used here. These peaks are the most significant wavelength and amplitude components in the input data, thus their number indicate how many different wavelengths there are, and their magnitude indicates the amplitude of the input wave. From these plots, it is possible to quantify the number and magnitude of different wavelengths as well as the bedform amplitudes.

4.2   2-D Fourier transform

Applying the Fourier transform to 1-D data still relies on the accurate selection of a 1-D profile. To address this issue, the 2-D Fourier transform can be used instead. As in the 1-D Fourier transform, the seabed height and wavelength are calculated, but in addition, the orientation the bedforms on the bed is too. The 2-D Fourier transform performs two 1-D Fourier analyses in both x and y where the results are plotted as Kx, Ky and normalised power. This distribution can be used to identify a bimodal orientation distribution, or multiple wavelength and height components with estimates of error in all measurements, based on measured variability and theoretical limits imposed by the Nyquist frequency of a data set. Given a synthetic bed with 20 m wavelength, 4 m amplitude and 60° orientated bedforms (Figure 4), the results of the 2-D Fourier transform is shown in Figures 6b and c.

As was the case with the 1-D Fourier transform, there are two peak values identified, whose wavenumber is 0.05 m. In addition to the information on the wavelength, there is also an orientation associated with the results. Rotating about the origin of the plot at $0, 0$ and starting from vertical ($x = 0$), the orientation is the angle from vertical to the peak value. In this instance, the position of the peak in Figure 6c is 60° from vertical, which is perpendicular to the orientation of the input data.

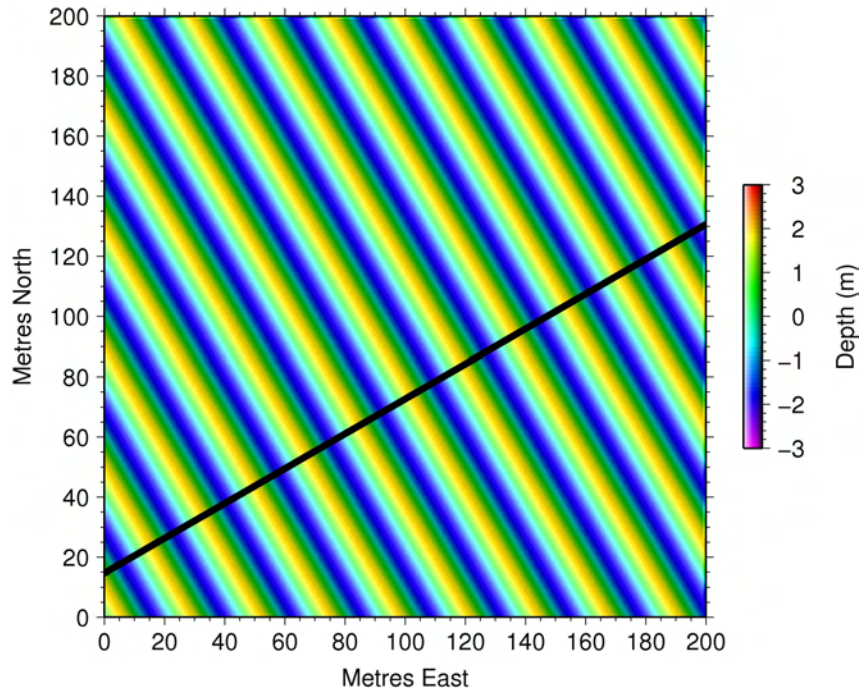Figure 4: Synthetic 2-D seabed surface with bedforms of wavelength 20 m, amplitude of 4 m and orientation of 60°. Black line indicates location of transect taken to generate Figure 5a.

Where the technique is most powerful is in extracting multiple orientations and wavelengths from a single input data set. Figure 7 shows a synthetic seabed with multiple input wavelength summed into a single bed. A traditional interpretation of the orientation of these synthetic bedforms might be of a long wavelength (∼50 m), low amplitude (∼4 m) series of bedforms normal to a more regular, ∼20 m and ∼8 m height series orientated 150° from north. Applying the 2-D Fourier transform to these data results in the power spectrum distribution shown in Figure 8. This analysis shows us that there are two distinct orientations, but that they are much closer than identified through the traditional interpretation. As input to the synthetic data, two bedform types were used: one dominant type was orientated 150° from north, with an amplitude of 4 m and a wavelength of 20 m; the second bedform type was orientated 75° from north, with an amplitude of only 2 m and a wavelength of 20 m. These two were summed, and the result is the surface shown in Figure 7.

Figure 8 shows the results of the 2-D Fourier transform on the bimodal bedform orientation surface where there are two clearly identifiable different orientation peaks. This shows how this quantitative approach reveals the limitations of a qualitative interpretation. When applied to real data, the power spectral plots reveal much more complex structures on the bed, with any number of discrete orientations. At present, the code is designed to generate a single mean orientation with estimates of variability based on a standard deviation of all the measured orientations.

4.3 2-D Fourier transform of bathymetric data

Figure 9 shows the results of applying the 2-D Fourier transform to a real bathymetric surface. The vector results are calculated over 35 m wide square patches of the seabed. The vectors are scaled to four times the calculated wavelength, the black vectors represent the mean wavelength and the white vectors the standard deviation.

The results show the general uniformity of the seabed, but also highlight how the orientation shifts from one subset to the next. Vectors with large errors associated with them are generally those whose standard deviation has encompassed a number of different bedform orientations.
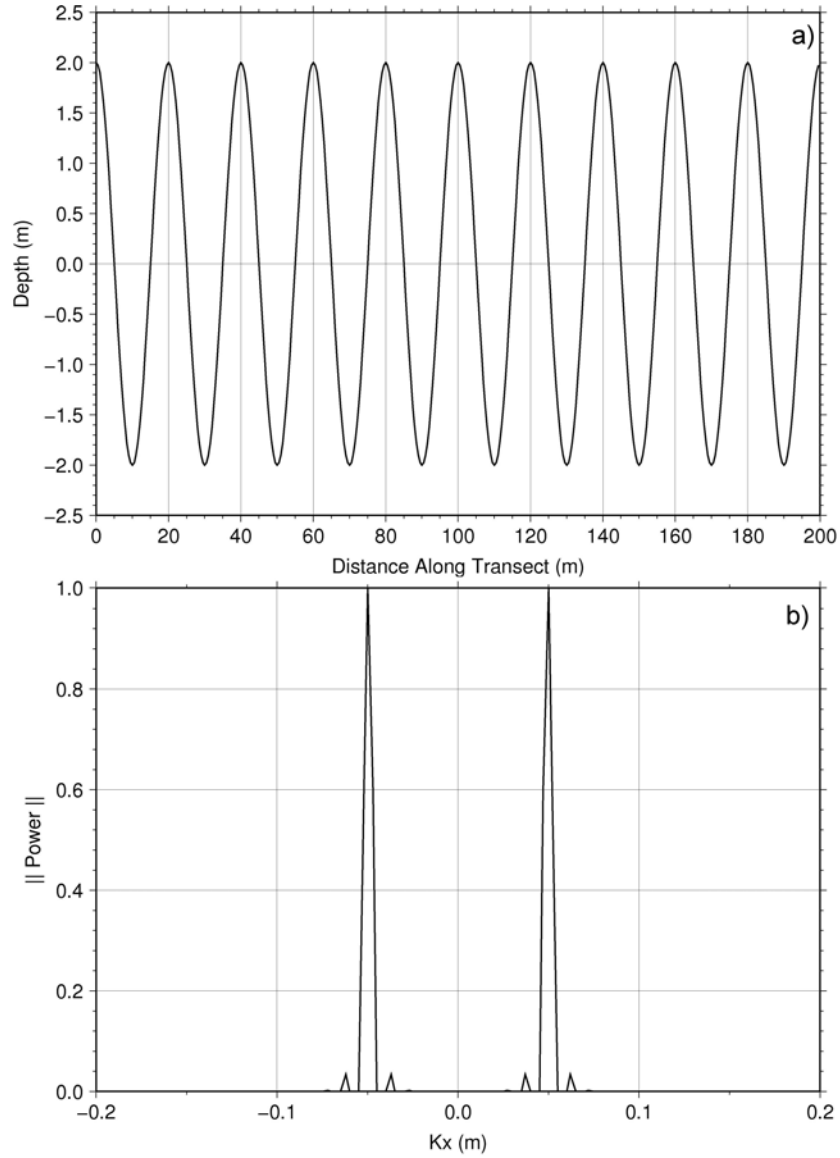
7

Figure 5: a) Synthetic bedform 2-D transect with a wavelength of 20 m and a height of 4 m. b) Normalised power for the 1-D Fourier transform of the sine wave synthetic bed shown in a). A threshold normalised power value of 0.6 (60%) is used to identify the main amplitude and wavelength of the input data.
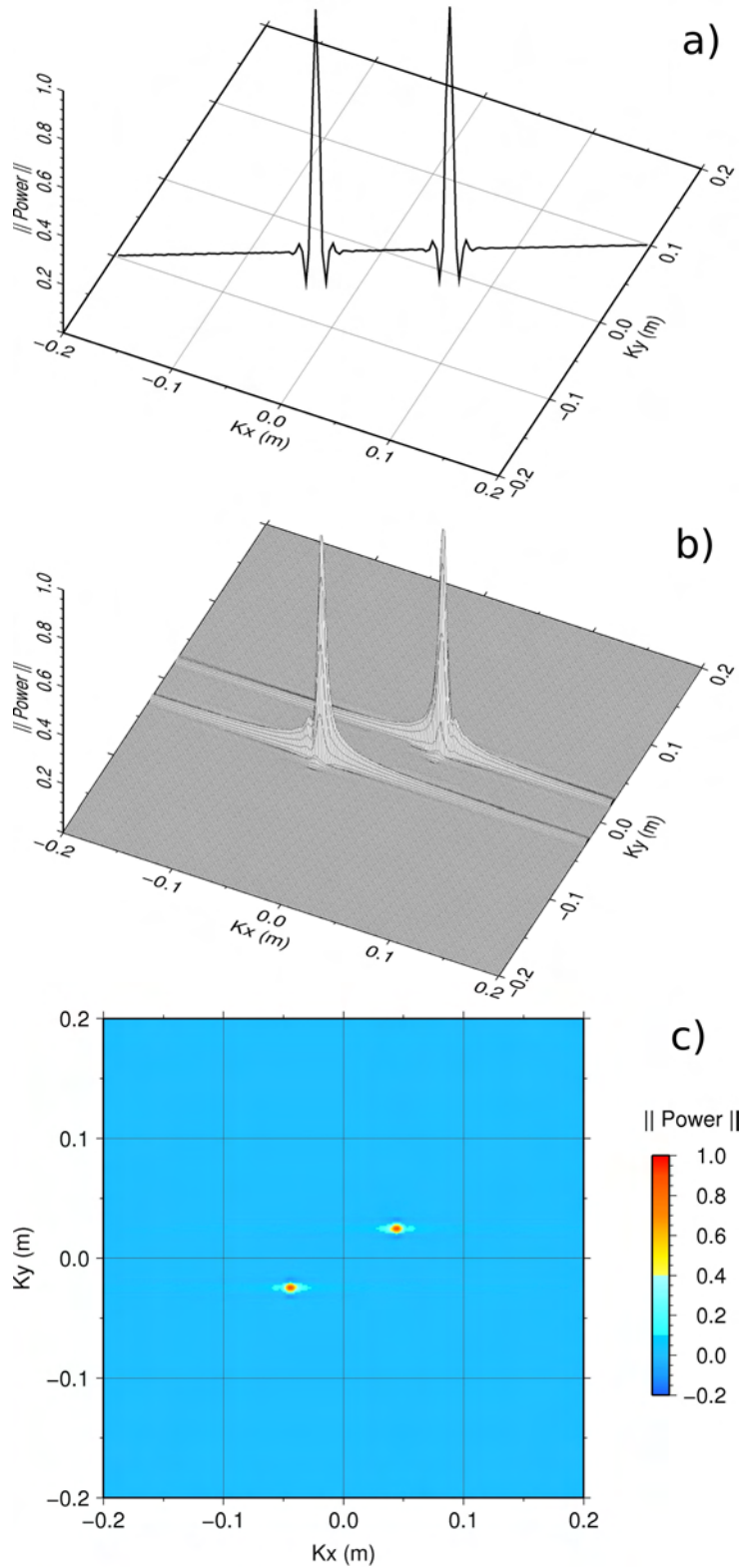
Figure 6: The transition from a 1-D Fourier transform to the power spectral density plots used to calculated bedform orientation, amplitude and wavelength. a) The result of the 1-D Fourier transform (Figure 5b) plotted on a 3-D axis. b) The 2-D Fourier transform of the 2-D synthetic surface (Figure 4). c) The 2-D Fourier transform plotted from above, with normalised power plotted using a colour scale.
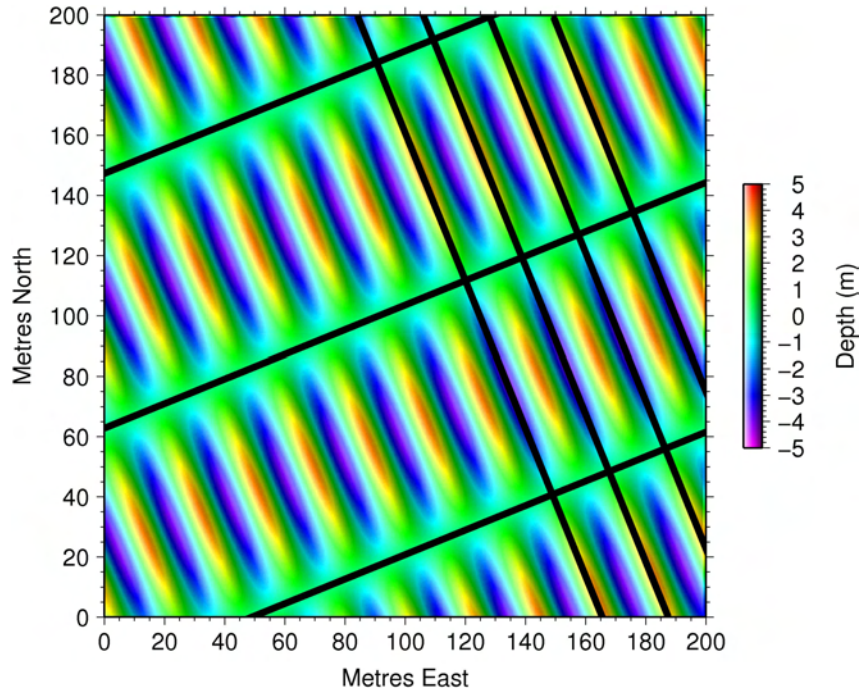
Figure 7: Synthetic 2-D seabed surface with multiple bedform orientations, but constant wavelengths and amplitudes. Black lines indicate qualitative interpretation of the surface: one bedform series of orientation 150° from north, and another normal to that (∼60°).
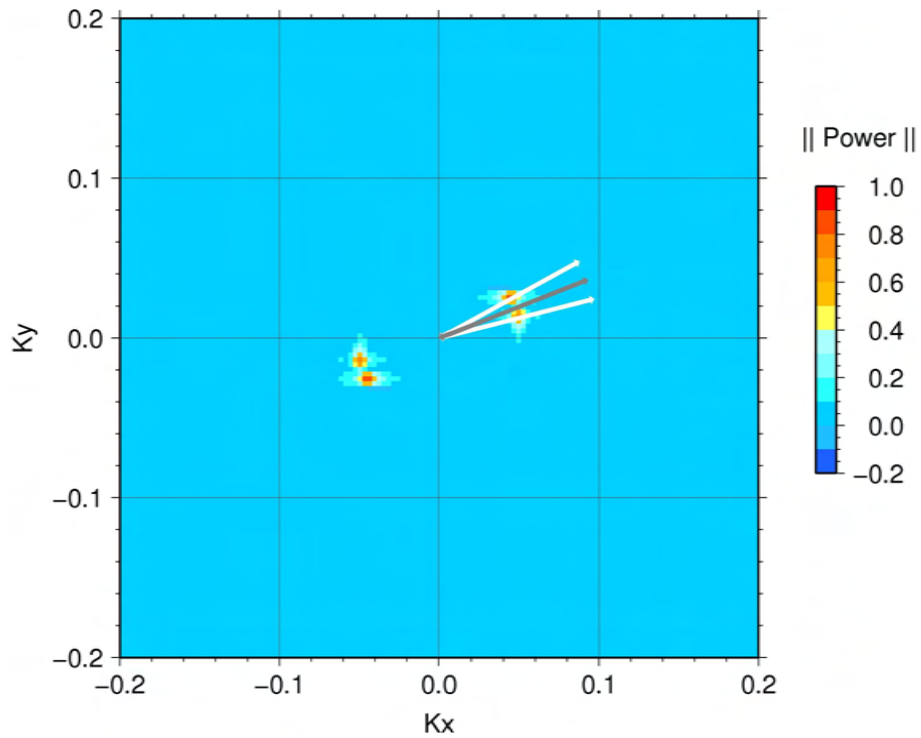

Figure 8: Normalised power spectrum density for the 2-D Fourier transform of the sine wave synthetic bed shown in Figure 7. Clearly visible are two distinct, yet close bedform orientations. The grey vector indicates the mean angle normal to bedform orientation, and is scaled to double the calculated wavelength. The white vectors are the standard deviation of the power values above 60% of the peak power.

The trend of a number of these particular vectors coincides with the edges of individual track lines, thus the multiple bedform orientations identified by the code are likely to be the artefacts in the edge beam overlap.
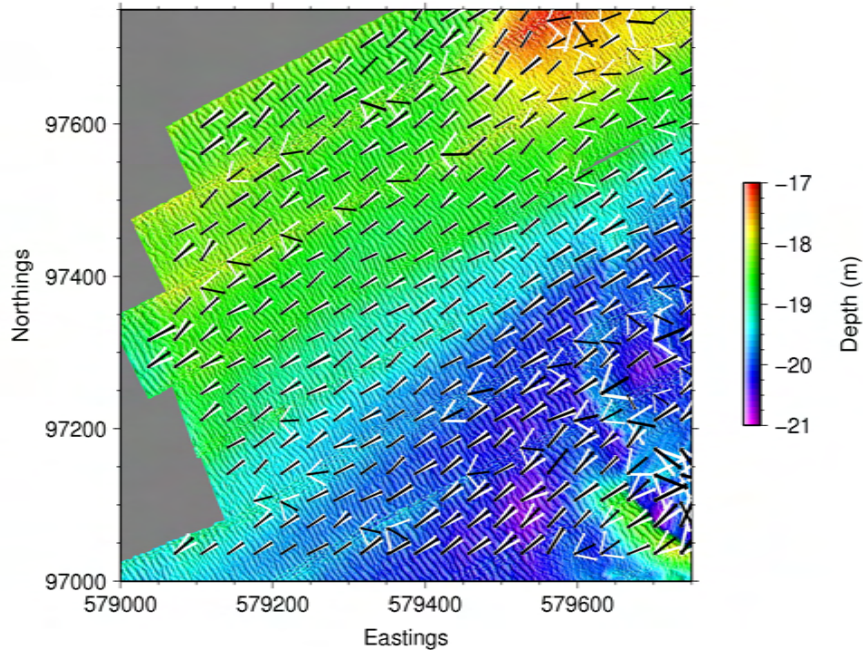

Figure 9: Swath bathymetry surface of part of the Hastings shingle bank. Calculated bedform orientation and wavelength depicted in the vector orientation and length respectively for 35 m subsets. White vectors indicate standard deviation of the picked power spectrum density for each subset region.

5   Discussion

The technique described herein holds promise for the quantification of bedforms on the seabed. A simple analysis using tools common to most GIS software packages can provide a first level of quantitative, objective analysis from which to further analyse a data set. In addition, a Fourier transform based approach gives further improvement in both spatial refinement, but also in the confidence of the results. The technique has been tested on a number of synthetic data sets of known parameters to ensure the results are accurate. The focus has been on obtaining the orientation and wavelength of a bedform field, but the Fourier transform can also generate wave amplitudes. At present, it is possible to split a large domain into a number of smaller regions, and obtain single mean values for each sub-domain.

Of particular interest to the authors is the possibility of extracting multiple orientations from each sub-domain, and using statistical analysis to determine the most significant of these. Comparison with a number of other hydrodynamic, geophysical and geotechnical data sets may provide further insights into the relationship between sediment transport and the associated flow-transverse bedform orientation.

6   Acknowledgements

thanks go to Mark Vardy for help with various aspects of the Fourier transform.

References

G. M. Ashley. Classification of large-scale subaqueous bedforms: a new look at an old problem. *Journal of Sedimentary Geology*, 60(1):160–172, 1990.

Y. A. Cataño-Lopera and M. H. García. Geometry and migration characteristics of bedforms under waves and currents. Part 1: Sandwave morphodynamics. *Coastal Engineering*, 53: 767–780, 2006.

P. G. Challenor, P. Cipollini, and D. Cromwell. Use of the 3D radon transform to examine the properties of oceanic Rossby waves. *Journal of Atmospheric and Oceanic Technology*, 18: 1558–1566, 2001.

P. Cipollini, D. Cromwell, and G. D. Quartly. Observations of Rossby wave propagation in the northeast Atlantic with TOPEX/POSEIDON altimetry. *Advances in Space Research*, 22(11): 1553–1556, 1998.

P. Cipollini, P. G. Challenor, and S. Colombo. A method for tracking individual planetary waves in remotely sensed data. *IEEE Transactions on Geoschience and Remote Sensing*, 44 (1):159–166, 2006.

J. P. Davis, D.J. Walker, M. Townsend, and I. R. Young. Wave-formed sediment ripples: Transient analysis of ripple spectral development. *Journal of Geophysical Research*, 109, 2004. doi: 10.1029/2004JC002307.

M. J. de Smith, M. F. Goodchild, and P. A. Longley. *Geospatial Analysis - A Comprehensive Guide to Principles, Techniques and Software Tools*. Matador, Second edition, 2007.

R. Dickson and A. Lee. Gravel extraction: effects on seabed topography. *Offshore Services*, 6: 32–39 and 32–39, 1973.

N. T. L. Grochowski, M. B. Collins, S. R. Boxall, and J. C. Salomon. Sediment transport predictions for the english channel, using numerical models. *Journal of the Geological Society of London*, 150:683–695, 1993.

R. J. O. Hamblin, A. Crosby, P. S. Balson, R. A. Chadwick, I. E. Penn, and M. J. Arthur. *The geology of the English Channel*. British Geological Survey UK Offshore Regional Report. Her Majesty's Stationary Office for the British Geological Survey, 1992.

N. H. Kenyon. Sand ribbons of European tidal seas. *Marine Geology*, 9:25–39, 1970.

N. H. Kenyon, R. H. Belderson, A. H. Stride, and M. A. Johnson. Offshore tidal sand banks as indicators of net sand transport and as potential deposits. *Special Publication of the International Association of Sedimentologists*, 5:257–268, 1981.

M. A. F. Knaapen, S. J. M. H Hulscher, and H. J. de Vriend. A new type of sea bed waves. *Geophysical Research Letters*, 28(7):1323–1326, 2001.

M. A. F. Knaapen, C. N. van Bergen Henegouw, and Y. Y. Hu. Quantifying bedforms migration using multi-beam sonar. *Geo-Marine Letters*, 25:306–314, 2005.

N. C. Mitchell and J. E. Hughes Clarke. Classification of seafloor geology using multibeam sonar data from the scotian shelf. *Marine Geology*, 121:143–160, 1994.

D. M. Rubin and R. E. Hunter. Bedform alignment in directionally varying flows. *Science*, 237: 276–278, 1987.

D. M. Rubin and H. Ikeda. Flume experiments on the alignment of transverse, oblique, and longitudinal dunes in directionally varying flows. *Sedimentology*, 37:673–684, 1990.

A. H. Stride, editor. *Offshore tidal sands: processes and deposits.* Chapman and Hall, 1982.